Published by
NIGERIAN SOCIETY OF PHYSICAL SCIENCES
Available online @ https://asr.nsps.org.ng/index.php/asr

African Scientific Reports 2 (2023) 82

African Scientific Reports

Isolation and Characterisation of High Grade Nanosilicon from Coastal Landform in Ilaje Local Government Area of Ondo State, Nigeria.

S. S. Oluyamo, O. F. Famutimi*, M. O. Olasoji

Department of Physics, Federal University of Technology, Akure, Nigeria.

Abstract

The application of silicon and silicon based materials in industries and optoelectronic devices cannot be over emphasized due to their unique properties. The availability of high grade silicon has been subject of interest for manufacturers and industrialist as the material has from discovery been very much insufficient to cater for the numerous demands for different uses and utilization. Numerous efforts have been put together to adapt the properties of silicon through the manufacture and fabrication of semiconductor compounds to replace silicon in functionality. Notwithstanding, the quest for more silicon in the environment is yet unabated. This research centers on the isolation and characterisation of high grade nanosilicon from coastal landform in Ilaje Local Government Area of Ondo State, Nigeria due to the attractive nature of the landforms in terms of colour and texture. Sand from the selected study area were categorised into different forms according to their colour and silicon isolated using the magnesiothermic reduction while the nanosilicon was obtained using an appropriate ball milling process. The morphology of nanosilicon from Zion, Micheal-Ugbonla, and Oluwa Glass coastal landforms shows an agglomeration of particles with irregular shapes having average particle sizes of 58.98 nm, 77.82 nm, and 37.27 nm, respectively. The XRD spectra of the nanosilicon showed sharp, distinct peaks that indicate crystallinity of the samples. The percentages of nanosilicon value obtained ranges from 65.23%-80.30% and considered high enough to find specific useful industrial applications in lithium ion batteries, biomedical devices, optoelectronic device utilization and computer industries.

DOI:10.46481/asr.2023.2.1.82

Keywords: Coastal landform, Magnesiothermic reduction, Nanosilicon, Characterisation

Article History :
Received: 04 January 2023
Received in revised form: 18 February 2023
Accepted for publication: 23 February 2023
Published: 15 March 2023

Communicated by: Wasiu Yahya

*Corresponding author tel. no: +2348068356341
Email address: famutimiolalekan@yahoo.com (O. F. Famutimi)

1. Introduction

Silicon is a metalloid and one of very few elements that have properties of both metals and non-metals. In nature, silicon can be found as either silica (quartz, sand) or silicates (feldspar, kaolinite). The production of computer chips, transistors, integrated circuits, solar cells, and automotive all often utilize silicon. Due to their unique optoelectronic properties, silicon nanoparticles have recently attracted the attention of various industries. In the bulk state, research indicate that silicon nanoparticles exhibit effective visible photoluminescence attributed to quantum confinement resulting from a reduced particle size smaller than the excitonic Bohr radius and their higher surface area to volume ratio [1, 2]. The worldwide demand for potential uses for nanosilicon serves as a significant driving force to reduce the size of silicon materials to the nanometer range [3, 4]. Quantum confinement has a substantial impact on silicon's performance and properties when its size is reduced to the 1-100 nm range [5]. Nanostructured materials have electrical, magnetic, and chemical properties that are significantly different from those of the corresponding bulk materials due to the reduced size of their basic building blocks. In comparison to bulk materials, nanostructured materials have been discovered to have increased strength and hardness, higher electrical resistivity, enhanced diffusivity, reduced density, etc. Bulk silicon has limited optoelectronic applications due to the indirect nature of its band gap. However, the development of nanostructured silicon has opened up a wide range of potential applications [6–8]. The best material for high density electronics is nanosilicon. The most effective method for converting silicon into a photonic material is by nanostructuring. The small size results in new quantum phenomena that yield extraordinary properties. Materials properties change drastically at the Nano scale because quantum confinement effects arise from the confinement of electrons and holes in the material. Additionally, at the Nano scale, short-range forces like van der Waals forces are dominant [9, 10]. As prospective low-cost emitters for optoelectronics, silicon nanoparticles have drawn a lot of interest. Nanosilicon can be utilized as an anode material of Li-ion batteries (LIBs) with the highest gravimetric capacity (4200 mA h g^{-1}) among anode candidates created up to this moment, which is a highly probable application. There have been several attempts to use nanostructured silicon for LIB applications in order to overcome silicon's drawbacks, such as volume expansion, pulverization, and evolving electrolyte decomposition, which are in fact observed with macro-sized silicon materials under repeated charge/discharge cycles [11–13]. The use of nanosilicon (Si) is the most promising routes for boosting the capacity of modern Li-ion batteries. Rechargeable Li-ion batteries (LIBs) offer a great energy storage solution for clean transportation, local energy storage systems, portable power and electronic devices [14].

The basic method of producing metallurgical silicon is through carbothermal reduction, which uses electric arc furnaces that operate at temperatures above 2000 ^{o}C [15]. However, silicon is liquefied during this energy-intensive process, which also destroys the SiO_2 original morphology. Magnesiothermic reduction has received attention recently because of its significantly lower operating temperatures (650 ^{o}C). It is possible to sufficiently accommodate the strain and prevent fracture by reducing silicon to the nanoscale [16–19]. Various researches have been carried out on extraction of elemental silicon using different materials like rice husk, sugarcane bagasse, corn cob as their starting material but there is little or no detailed information on the isolation of nanosilicon from any of these materials. Interestingly, the landform in the study areas have different colours and are used for limited agricultural and industrial purposes. Aside the fact that the sand in the area may contain high grade silicon, it is believed that the colour of the landforms would have effect on the silicon contents. It is hoped that studies on the isolation and characterisation of nanosilicon will increase the industrial value of the landforms. In addition, the research will serve as a data base for the development of new approaches in converting landforms to useful applications as well as provide available source of high grade silicon/nanosilicon for industrial applications.

2. Experimental Details

2.1. Collection of samples

The sand samples used in the analysis were collected from different coastal landforms in Ilaje Local Government Area of Ondo State, Southwestern Nigeria. The samples were collected at a depth of about 30 cm from the surface into non-reacting polyethylene bags. The sources and location of the areas where the samples were collected are presented in Table 1.

2.2. Theoretical Background

The interplanar spacing (d-spacing) was determined using the Bragg equation [20, 21]:

$$n\lambda = 2d sin\theta, \tag{1}$$

where n is the order of reflection, λ is the wavelength of the incident X-ray (m), d is the interplanar spacing of the crystal, and θ is the Bragg's angle (°).

Scherrer's equation was used to calculate the crystallite size (L). It is given as:

$$L = \frac{K\lambda}{B\cos\theta}, \tag{2}$$

where K is a constant value given as 0.91, the incident X-rays' wavelength is λ, the Bragg's angle (°) is θ, the intensity of the Full Width at Half Maximum (FWHM) proportional to a high intensity peak of the diffraction plane is B.

2.3. Preparation of samples

Fifty (50) grams of each sand sample was washed successively with 250 ml of 1 M hydrochloric acid (HCl) at a temperature of 75 °C and 1 M sodium hydroxide (NaOH) at room temperature for 3 hours. Distilled water was used after each step to remove any trace of acid and alkali. The washed sample was dried in an oven at 105 °C for 2 hours. A mechanical test sieve shaker was also used to sieve the sand samples into 63 µm for a homogenous size distribution at the Department of Metallurgical and Materials Engineering, Federal University of Technology, Akure.

Table 1. Sources/ Area Covered with their Position Using Global Positioning System (GPS)

Coastal Landforms	Sources	Colour	Longitude (°E)	Latitude (°N)
Zion	Zion Igbokoda, Ilaje LGA	White	004.80807	06.35184
Micheal Ugbonla	Micheal Ugbonla Street, Ilaje LGA	White	004.73048	06.14870
Oluwa Glass	Oluwa Glass Checking point, Igbokoda, Ilaje LGA	Brown	004.77157	06.39092

2.4. Magnesium reduction of the silica and synthesis of nanosilicon

16.0 g of sand (silica) and 15.0 g of magnesium powder (180 µm) were mixed thoroughly for effective reaction to take place. This was subsequently transferred to platinum crucible and heated at a temperature of 800 °C for 30 minutes [22, 23]. The samples were then allowed to cool down gradually to room temperature. The equation of reaction is given as:

$$SiO_2(s) + 2Mg(s) \rightarrow 2MgO(s) + Si(s). \tag{3}$$

When silica is heated with magnesium powder, MgO and Si are formed. The unreacted Mg and its products is completely removed by washing one gram (1 g) of silicon (Si) sample using 20 ml of 5 M HCl at 100 °C and stirring using a magnetic stirrer for 60 minute for effective leaching to take place. The hydrochloric acid leached product was washed thoroughly with distilled water. The washed Si samples are then dried in an oven at 105 °C for 5 hours and stored in desiccator. Dried silicon particle were ball-milled into nanoparticle by using high energy ball- mill. The isolated nanosilicon was analysed using EDX, SEM (JOEL-JSM 7600F NanoSEM equipment) and XRD (using GBC EMMA XRD equipment, Australia)

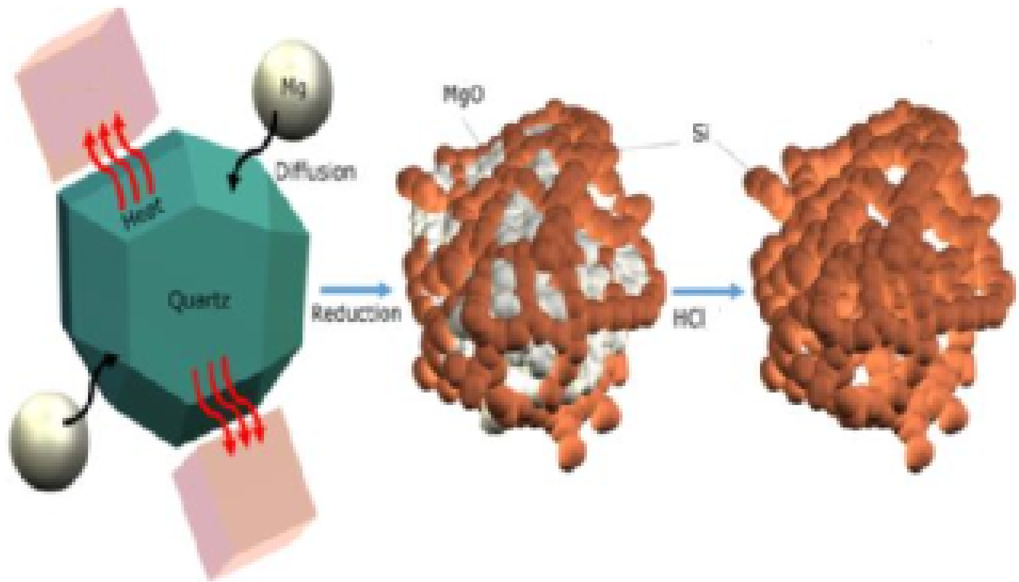

Figure 1. Schematic Diagram of Magnesium reduction of the silica (Quartz)

3. Results and Discussion

3.1. X-ray Diffraction (XRD) Analysis

As shown in Table 2, the values of interplanar spacing (d-spacing) and band position of angle 2-Theta (2 θ) in the nanosilicon spectra closely matched those reported in the International Centre for Diffraction Data (ICDD). Well-oriented and distinct crystalline peaks were obtained, as shown in Figures 2-4. It was noticed that the silica had a pronounced peak in the sample. This could be due to the powder's contact with air, especially during storage. Also, the presence of oxygen, which could be caused by silica that was not removed via HCl leaching [24]. Table 2 shows the band position (2θ), FWHM, crystallite size, and d-spacing of nanosilicon. Calculations using Scherrer's equation (2) revealed that the sizes of crystallite were 48.34 nm, 51.92 nm, and 23.89 nm for Zion, Micheal-Ugbonla, and Oluwa glass coastal landforms, respectively. XRD patterns of the nanosilicon for the coastal landforms revealed that the diffraction peak planes are in good agreement with the International Centre for Diffraction Data (ICDD), as shown in Table 2.

Table 2. Band position (2θ), FWHM, Crystallite size and d-spacing of Nanosilicon

Coastal Landforms	2θ	FWHM (β) (rad)	Crystallite Size (nm)	D-Spacing d (A^0)	Ref. Code Marching (ICDD)	
					Silicon	Synthesis Quartz (SiO_2)
Zion	28.64	0.003030	48.3414	3.120000	00-027-1402	00-033-1161
Micheal-Ugbonla	28.62	0.002758	51.9239	3.120000	00-003-0544	01-083-2466
Oluwa glass	28.54	0.006056	23.8865	3.135500	00-027-1402	00-046-1045

3.2. Scanning Electron Microscopy (SEM) Analysis

As shown in Figures 5-7, the morphology of the nanosilicon for Zion, Michael–Ugbonla, and Oluwa glass coastal landforms revealed the existence of agglomerations of particles with irregular shapes having average particle sizes of

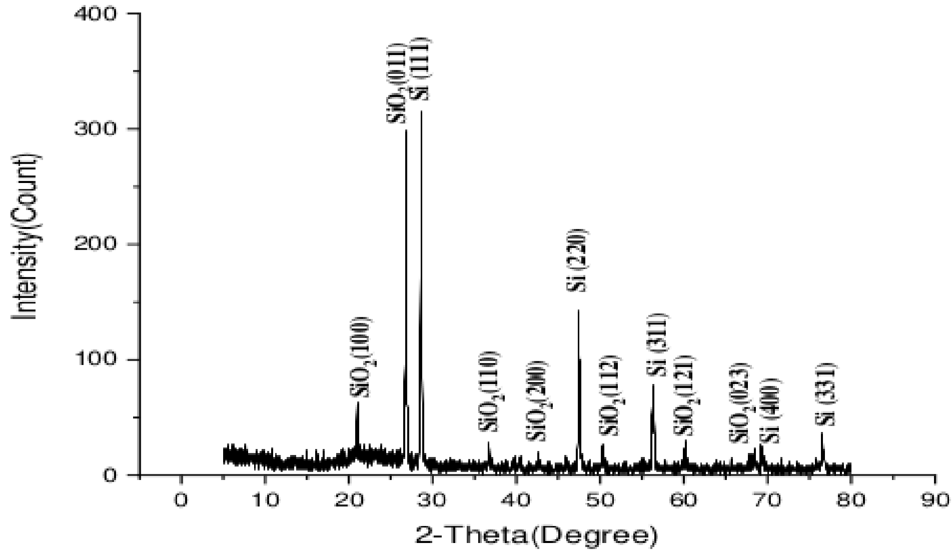

Figure 2. XRD pattern of nanosilicon of Zion coastal landform

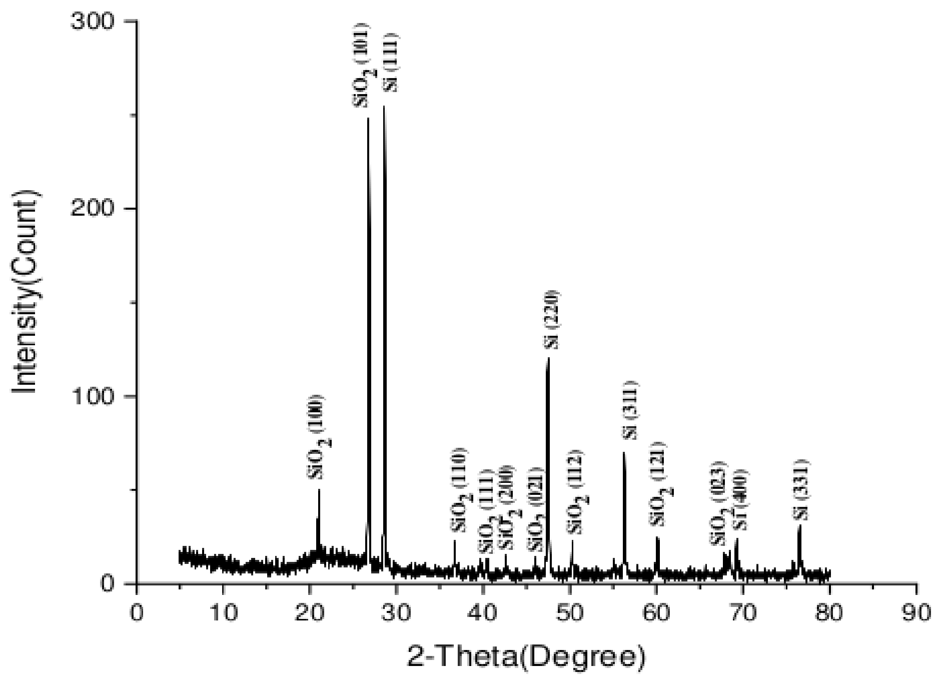

Figure 3. XRD pattern of nanosilicon of Micheal-Ugbonla coastal landform

58.98 nm, 77.82 nm, and 37.27 nm, respectively. The presence of agglomerates is an inevitable phenomenon that is associated with the interaction between particles of small size due to electrostatic attraction or van der Waals force [25]. The small size of the silicon nanoparticles obtained indicates that they can be usefully exploited in a suitable

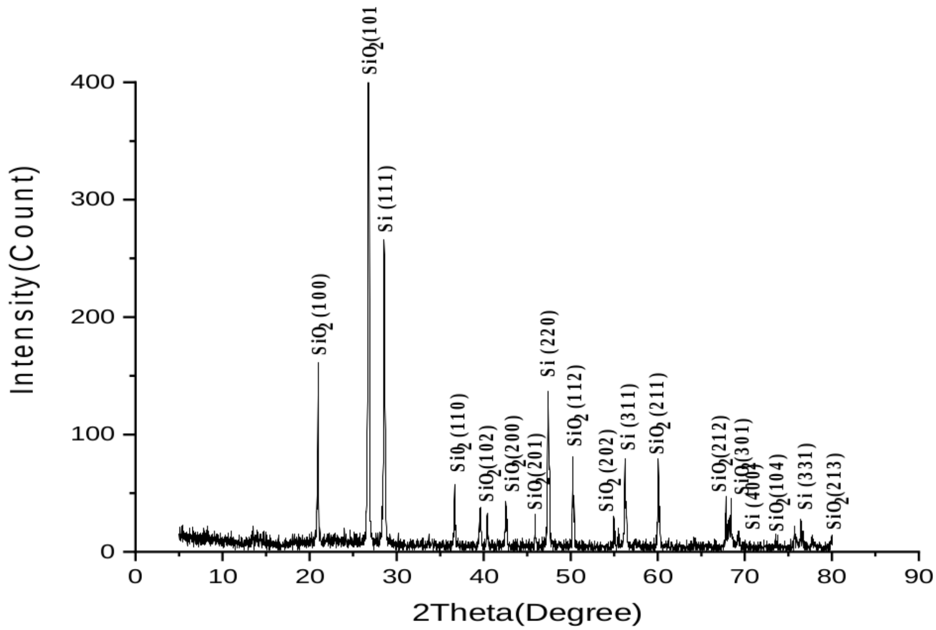

Figure 4. XRD pattern of nanosilicon of Oluwa glass coastal landform

application.

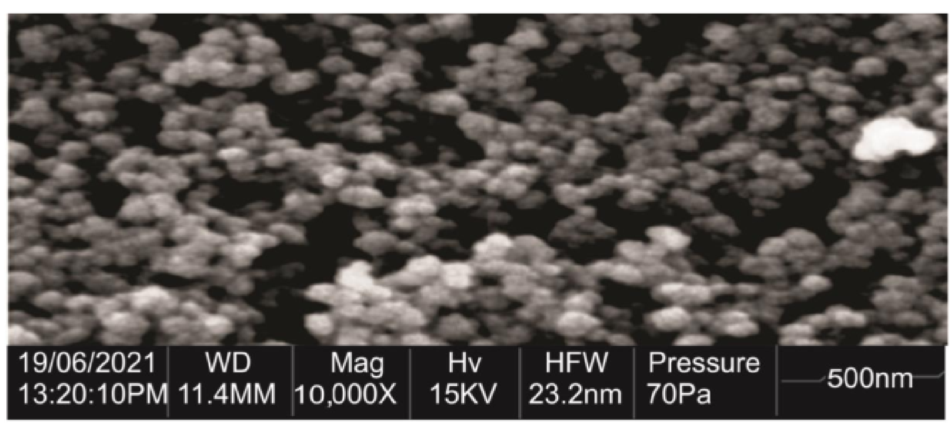

Figure 5. SEM image of nanosilicon of Zion coastal landform

3.3. Energy Dispersive X-ray (EDX) Analysis

The elemental composition of the raw samples from the coastal landform was determined by energy dispersive X-ray (EDX), as shown in Table 3. EDX indicates that silicon has the highest percentage among the elements observed in the spectra. Impurities in quartz sands like Na, K, Al, and Fe are presumed to emanate from minerals like mica and feldspar [26]. This range of silicon content (i.e., 58.60%–63.73%) in the raw samples as obtained from the respective sources (i.e., Zion, Micheal-Ugbonla, and Oluwa glass landforms) is considered relatively low for meaningful industrial utilization.

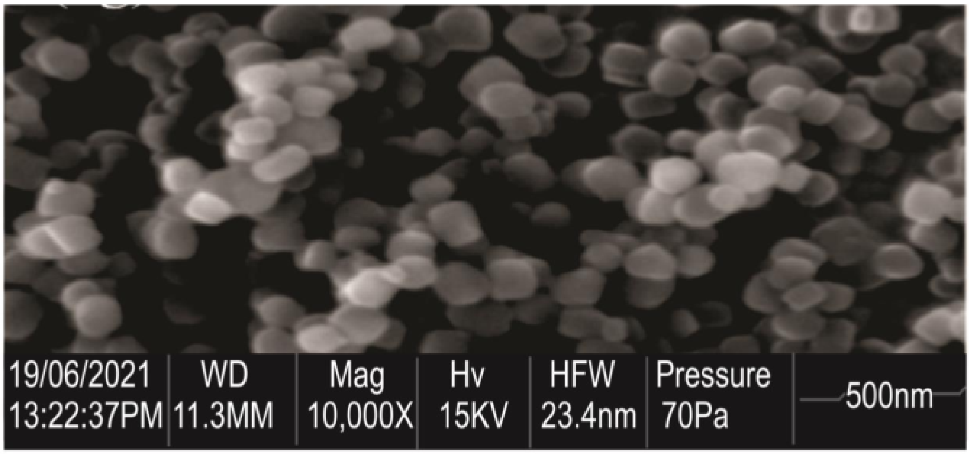

Figure 6. SEM image of nanosilicon of Micheal Ugbonla coastal landform

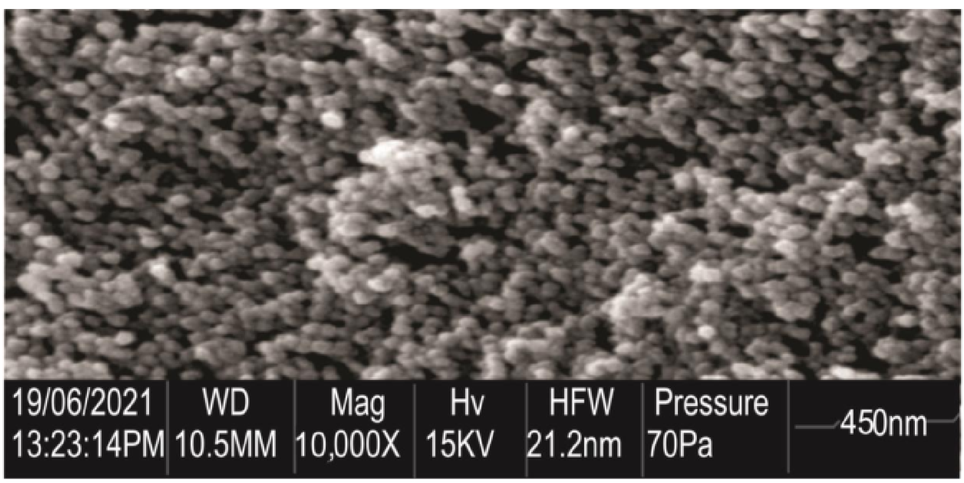

Figure 7. SEM image of the nanosilicon of the Oluwa Glass coastal landform

Element	Wt (%)
Si	80.30
Mg	2.52
C	3.20
O	7.00
Ca	1.31
Fe	2.10
S	0.05
Na	1.12
K	1.20
Al	1.20

EDS analysis

Figure 8. EDX of nanosilicon from the Zion coastal landform

However, the EDX analyses after the process of isolating nanosilicon revealed that the nanosilicon obtained from

Table 3. Result of EDX Analysis for the Raw Sample

Element (%)	Coastal Landforms		
	Zion	Micheal-Ugbonla	Oluwa glass
Si	58.60	63.72	60.60
Mg	0.35	1.32	0.35
C	5.20	0.24	4.20
O	10.30	10.30	15.30
Ca	3.34	3.25	3.33
Fe	3.50	6.52	3.52
S	-	-	-
Na	3.20	2.24	2.20
K	-	-	-
Al	15.40	9.10	10.40
Mn	0.11	1.10	0.10

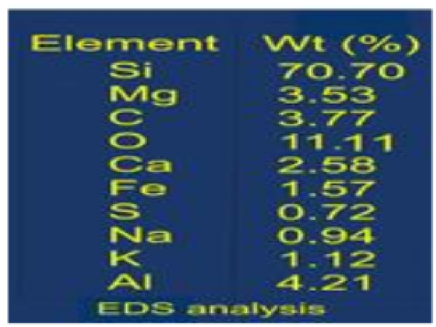

Element	Wt (%)
Si	70.70
Mg	3.53
C	3.77
O	11.11
Ca	2.58
Fe	1.57
S	0.72
Na	0.94
K	1.12
Al	4.21

EDS analysis

Figure 9. EDX of nanosilicon from the Micheal Ugbonla coastal landform

Element	Wt (%)
Si	65.23
Mg	4.52
C	3.85
O	10.83
Ca	3.68
Fe	3.92
S	0.69
Na	1.06
K	1.12
Al	5.10

EDS analysis

Figure 10. EDX of nanosilicon from the Oluwa Glass coastal landform

the samples ranged from 65.23% to 80.30%, as presented in Figures 8–10. The coastal landform obtained from Zion with a whitish colour had the highest percentage, while that obtained from Oluwa glass with a brownish colour had the lowest percentage value of nanosilicon. This could be due to the chemical composition of the samples, as earlier reported by [27]. These values are high enough and can find useful applications in material fabrication and industrial utilization. Although the percentages of all other elements in the landforms decreased considerably, the magnesium contents were found to increase. This could be due to the magnesium powder used as a reducing agent. The presence of metallic contaminants may have detrimental effects for some applications, such as solar cells, nonetheless, these metallic impurities may increase the conductivity of nanosilicon in battery applications [28, 29]. Sulphur and potassium were not noticed in the raw samples, their appearance in the isolated samples could have been injected into the materials via the EDX machine.

4. Conclusion

It was established in the research that the percentages of nanosilicon value obtained ranged from 65.23%-80.30% and were high enough to find useful industrial applications in areas like lithium ion batteries, biomedical devices, photovoltaic/solar cells, computer industries, etc. Silicon and oxygen were prominent among the samples characterized. In conclusion, the percentage of isolated nanosilicon from the coastal landform is pure enough to be further purified and used as a starting material for the production of semiconductor-grade silicon.

Acknowledgement

The authors gratefully acknowledge the Department of Chemistry and the Department of Metallurgical and Materials Engineering, Federal University of Technology, Akure, for allowing us to use the facilities in their laboratories during the period of the research. You are highly appreciated.

References

[1] H. Lin, C. P. Huang, W. Li, C. Ni, S. I. Shah & Y. H. Tseng, "Size dependency of nanocrystalline TiO_2 on its optical property and photocatalytic reactivity exemplified by 2-chlorophenol", Applied Catalysis B: Environmental **68** (2006) 1.

[2] A. Momeni & M. H. Mahdieh, "Photoluminescence analysis of colloidal silicon nanoparticles in ethanol produced by double-pulse ns laser ablation", Journal of Luminescence **176** (2016) 13.

[3] R. Koole, E. Groeneveld, D. Vanmaekelbergh, A. Meijerink & C. M. Donegá, "Size effects on semiconductor nanoparticles", Springer, Verlag Berlin Heidelberg **1** (2014) 13.

[4] M. I. Baig, P. G. Ingole, W. K. Choi, J. D. Jeon, B. Jang, J. H. Moon & H. K. Lee, "Synthesis and characterization of thin film nano composite membranes incorporated with surface functionalized silicon nanoparticles for improved water vapor permeation performance", Chemical Engineering Journal **308** (2017) 27.

[5] D. S. Klaus, *Silicon nanomaterials source book low-dimensional structures, quantum dots, and nanowires*, CRC press Taylor & Francis group, (2017).

[6] T. Makino, M. Inada, K. Yoshida, I. Umezu and A. Sugimura, "Structural and optical properties of silicon nanoparticles prepared by pulsed laser ablation in hydrogen background gas", Applied Physics A **79** (2004) 1391.

[7] M. H. Wua, R. Mu, A. Ueda, D. O. Henderson, B. Vlahovic, "Production of silicon quantum dots for photovoltaic applications by picosecond pulsed laser ablation", Materials Science and Engineering B **116** (2005) 273.

[8] J. H. Kim, K. A. Jeon, G. H. Kim and S. Y. Lee, "Optical properties of silicon nanocrystalline thin films grown by pulsed laser deposition", Optical Materials **27** (2005) 991.

[9] J. L. Yeh, H. L. Chen, A. Shih and S. Lee, "Formation of Si nanoclusters in amorphous silicon thin films by excimer laser annealing", Electronics Letters **35** (1999) 23.

[10] M. H. Wu, R. Mu, A. Ueda and D. O. Henderson, "Properties of Silicon Nanoparticles Produced by Picosecond Pulsed Laser Ablation", Materials Research Society sympodium proceedings **638** (2001) 1.

[11] C. K. Chan, H. Peng, G. Liu, K. McIlwrath, X. F. Zhang, R. A. Huggins and Y. Cui, "High-performance lithium battery anodes using silicon nanowires", Nature nanotechnology **3** (2008) 31.

[12] B. Hertzberg, A. Alexeev and G. Yushin, "Deformations in Si-Li Anodes Upon Electrochemical Alloying in Nano-Confined Space", Journal of the American chemical society **132** (2010) 8548.

[13] L. F. Cui, L. Hu, H. Wu, J. W. Choi and Y. Cui, "Designing nanostructured Si anodes for high energy lithium ion batteries", Journal of The Electrochemical Society **158** (2011) A592.

[14] M. Tarascon, M. Armand, "Issues and challenges facing rechargeable lithium batteries", Nature **414** (2001) 359.

[15] B. G. Gribov & K. V. Zinov'ev, "Preparation of High_purity Silicon for Solar Cells", Journal of Inorganic Materials **39** (2003) 653.

[16] C. K. Chan, "High-performance lithium battery anodes using silicon Nanowires", Nature Nanotechnology **3** (2008) 31.

[17] H. Wu, "Stable cycling of double-walled silicon nanotube battery anodes Through solid-electrolyte interphase control", Nat. Nanotechnol. **7** (2012) 310.

[18] X. H. Liu, "Size-Dependent Fracture of Silicon Nanoparticles During Lithiation" American Chemical Society Nano **6** (2012) 1522.

[19] H. Wu & Y. Cui, "Designing nanostructured Si anodes for high energy lithium ion batteries" Nano Today **7** (2012) 414.

[20] U. J. Kim, S. H. Eom, & M. Wada, "Thermal decomposition of native cellulose: Influence on crystallite size", Polymer Degradation and Stability **95** (2010) 778.

[21] M. Wada & T. Okano, "Localization of Iα and Iβ phases in algal cellulose revealed by acid treatments", Cellulose **8** (2001) 183.

[22] A. Onajah, A. N. Amah & Ayomanor, "Comparative studies of silicon from rice husk ash and natural quartz", American Journal of Scientific and Industrial Research **3** (2012) 146.
[23] M. D. Vazeed, J. Akash, M. Anusha, & V. K. Ajay, "Quantitative and Qualitative Analysis of Silicon extracted from Godavari river sand, Kandakurthi, Telangana, India", International Journal of Engineering Research & Technology (IJERT) **4** (2015) 2278.
[24] A. Darghouth, S. Aouida & B. Bessais, "High Purity Porous Silicon Powder Synthesis by Magnesiothermic Reduction of Tunisian Silica Sand", Silicon **13** (2021) 667.
[25] A. Ruksudjarit & G. Rujijanagul, "Synthesis of SiO_2 nanopowder from rice husk ash", Advanced Materials Research **55** (2008) 649.
[26] G. Dal Martello, E. Tranell, S. Gaal, O. S. Raaness, K. Tang & L. Arnberg, "Study of Pellets and Lumps as Raw Materials in Silicon Production from Quartz and Silicon Carbide", Metallurgical and Materials Transactions B. **42b** (2011) 939.
[27] C. Victor & R. Alvaro, "Measure of the colour of beach nourishment sands: A case study from Belgium coast", Article in Trabajos de Geologia, Universidad de Oviedo **35** (2015) 7.
[28] A. Waqar, R. A. Majid, Y. Zhichun, K. Jahangeer, J. Wenkui, J. Fan, C. Liang, L. Nishuang, L. Luying & G. Yihua, "Extraction of nano-silicon with activated carbons simultaneously from rice husk and their synergistic catalytic effect in counter electrodes of dye-sensitized solar cells", Scientific Reports **6** (2016) 39314.
[29] F. Zachary, W. Wei, H. B. Hamed, M. Zafer, A. Kazi, L. Chueh, O. Mihrimah & S. O. Cengiz, "Scalable synthesis of nano-silicon from beach sand for long cycle life Li-ion Batteries", Scientific Reports **4** (2014) 5623.